95121

LA-UR- 98-1524

*Approved for public release; distribution is unlimited.*

Title: Optical Imaging Through Turbid Media Using a Degenerate-Four-Wave Mixing Correlation Time Gate

RECEIVED
OCT 05 1998
OSTI

Author(s): Irving J. Bigio, CST-4
Charlie E.M. Strauss, CST-1,
David K. Zerkle, CST-6

Submitted to: DOE Office of Scientific and Technical Information (OSTI)



**Los Alamos**
NATIONAL LABORATORY

## DISCLAIMER

# Optical Imaging Through Turbid Media Using a Degenerate-Four-Wave Mixing Correlation Time Gate

Irving J. Bigio*, CST-4
Charlie E.M. Strauss, CST-1,
David K. Zerkle, CST-6

**Abstract**

This is the final report of a three-year, Laboratory Directed Research and Development (LDRD) project at the Los Alamos National Laboratory (LANL). We have demonstrated the use of a degenerate-four-wave-mixing time gate to allow imaging through turbid media, with potential application to tissue imaging. A near infra-red (NIR), long-pulse $Cr^{+3}$:$Li_2SrAlF_6$ laser was used as the light source (during most of the project) for imaging through clear and turbid media. Preliminary experiments were also carried out with a continuous diode laser.

## Background and Research Objectives

In the past several years much effort has been applied toward the development of optical tomography for applications such as mammography and brain imaging, motivated by the possibility of eliminating the use of ionizing radiation. The challenge results from the fact that tissues are strongly scattering, and the scattering coefficient can be a factor of 100 greater than the absorption coefficient, even in the optimal near infra-red (NIR) spectral region. For two-dimensional imaging, a variety of schemes have been investigated for time gating to selectively detect ballistic photons (i.e. photons that are not scattered) and quasi-ballistic, or "snake" photons (photons that undergo very little scattering and stay on a predominantly straight path between the source and the detector).

In addition to the conceptually straight forward electronic gating of the detector [1], Kerr-gate shuttering [2], collimation and spatial filtering [3], and coherent, nonlinear-optical, time-gating techniques such as stimulated Raman scattering (SRS) [4,5] and coherent anti-Stokes Raman spectroscopy (CARS) [6,7] are among several methods that have been proposed for this purpose. While many of these methods rely on ultrafast lasers, a few are based on correlation gates (which may be implemented, for example, for SRS or CARS). A correlation gate can be formed by the interference of two signals originating from the same laser. The length of the gate is determined by the coherence time of the laser. Therefore, methods employing broad bandwidth light for correlation time

* Principal Investigator, Irving J. Bigio: e-mail: ijb@lanl.gov

gates can use longer laser pulses, even continuous wave (cw) lasers. Technically, this may allow for lower-cost, more reliable systems.

Fundamentally, a potential advantage of long pulses or cw illumination is that for each exposure more light may illuminate the tissue since the peak powers are lower. This can be very important when a basic question is whether there are sufficient ballistic and snake photons to form an image, regardless of the noise rejection efficiency. The method described here, resonant degenerate-four-wave-mixing (DFWM), was first suggested by Feinberg [8], but to our knowledge no experimental demonstrations have been published prior to our work [9]. DFWM covers a variety of nonlinear optical phenomena, and may be used as a correlation time-gate to produce an effective, ultrafast optical gate. The process is analogous to forming a holograph in the nonlinear medium, which is then read out in real-time. Electronic holography has previously been demonstrated as a method for imaging through biological tissues [10-12]. DFWM can take advantage of optical processes occurring on or very near resonant transitions in atoms or molecules, thus providing signal amplification. DFWM also offers, theoretically, the highest possible rejection of the diffuse light component. However, in practice, a variety of experimental issues determine the lower limits for the noise, which generally are considerably in excess of the theoretical limits.

## Importance to LANL's Science and Technology Base and National R&D Needs

Within the Laboratory's core mission program, the development of methods for imaging in turbid media has applications to the scientific stockpile stewardship program as a method of imaging within polymer components while measuring the properties of these materials from nuclear weapons. The development of minimally and noninvasive medical diagnostics is directly relevant to the Bioscience and Biotechnology core competency at the Laboratory, and healthcare technologies is an identified component of the Laboratory's Genome and Beyond tactical goal.

Nationally, the development of minimally invasive methods for breast cancer diagnostics is of relevance to several federal agencies including the National Institutes of Health, the Office of Women's Health and the Army Medical Research and Materiel Command, all of which have active programs in this area.

## Scientific Approach and Accomplishments

In initial experiments, a $Nd^{+3}$:YAG was used as the optical source [9]. However, for practical imaging through human tissue, the laser should operate in the NIR spectral region, where the tissue absorption is minimized, and the laser's peak intensity should lie below the tissue damage threshold. In view of these constraints, a $Cr^{+3}$:$Li_2SrAlF_6$ laser was chosen for the current experiments. In the gain-switched mode, the pulse duration lies in the range 30-40 μsec. Although this long pulse exhibits the typical spiking, peak powers are still orders of magnitude lower than those obtained in the Q-switched mode. The bandwidth is ≈3-4 nm when free-running, and ≈0.1-1.0 nm with the insertion of a single birefringent filter; the wavelength is typically in the range ≈830-840 nm. A schematic of the experimental apparatus is shown in Figure 1.

The output from this laser is polarized, spatially filtered, and split into a forward pump beam, $E_f$, and a probe beam $E_p$. The forward pump beam, $E_f$, is gently focused and directed through the nonlinear medium, in our case a dye solution in a cuvette [13,14]. The forward pump beam is retro-reflected to form the backward pump beam, $E_b$, whose polarization is rotated $90^o$ with respect to $E_f$ by double-passing through a $\lambda/4$ plate. $E_p$ enters the cuvette through the front face, and intersects the forward pump beam at an angle $\approx 15^o$. The optical delay line for $E_p$ includes a precision translation stage, which allows for 0.01 mm ($10^{-13}$ sec) resolution. The phase-conjugate signal, $E_s$, is generated when $E_b$ scatters off the volumetric grating formed by the interference of $E_p$ and $E_f$.

The signal is coupled out through a polarizing beam splitter, and directed onto a high sensitivity CCD camera. Polarizers and beam apertures are used throughout to reject scattered light and improve the signal-to-noise ratio. In DFWM, the signal is proportional to the induced nonlinear index in the medium, which can be a resonantly enhanced process. The path lengths of $E_f$, and $E_p$ are made equal, so that only ballistic and quasi-ballistic photons along the path of $E_p$ arrive coherently with $E_f$. Where $E_f$ and $E_p$ cross in the medium, a Bragg grating is formed by the interaction of the interference pattern with the medium. The backward-propagating pump beam, $E_b$, scatters off this grating directly back along the probe beam path, forming the signal, $E_s$, which is the phase conjugate of the probe beam, $E_p$.

The backward pump need not arrive at the same time as the two beams that formed the grating, nor does it have to be coherent with them, in order to "read out" the "hologram", as long as the grating is still present. In our experiment, the backward pump is actually delayed about 4 ns with respect to the beams that form the grating. Under the right circumstances the amplitude of $E_s$ can be greater than the original probe beam since the counter-propagating pump beams are much more powerful than the probe; thus, amplification can be achieved. Light delayed by multiple scattering in the phantom cannot form a grating with either pump, and therefore produces no periodic index variations from which the backward pump can scatter.

Images were taken of crosshairs, made from 300-μm-diameter wires, through both clear and scattering media, as shown in Figure 2. The scattering medium consisted of Intralipid-10% diluted by a ratio of 1:40 with deionized water; the pathlength through the cell was 1 cm. The crosshair was placed before the scattering cell, in the optical path of $E_p$. Intralipid is a phospholipid/water emulsion used as an intravenous nutrient. At 840 nm, the reduced scattering coefficient, $\mu_s'$, is about 84 $cm^{-1}$ for undiluted Intralipid-10% [15]. For a 1:40 dilution, this yields an effective value for $\mu_s'$ of 2 $cm^{-1}$. For human breast tissue at this same wavelength, $\mu_s'$ has been reported to be between approximately 2 $cm^{-1}$ and 12 $cm^{-1}$ [16] with the variation among the different constituents of breast tissue. Other investigators find a $\mu_s'$ value closer to 2 cm-1 for *in vivo* specimens of healthy breast tissue [17]. Thus our experimental scattering cell is roughly equivalent in scattering to a thickness of between 2 mm and 10 mm of breast tissue.

Several features were noted in this experimental arrangement. First the spatial resolution was much better horizontally than vertically. Figure 2 shows images of a crosshair obtained with our apparatus. The vertical wire is clearly observed, while only a hint of the horizontal wire can be detected in frames a) and d). We speculate that this may be due to the particular geometry we are using, in which the pump and probe beams cross in the horizontal plane. We are investigating this by examining a geometry in which the beams cross in a vertical, rather than horizontal plane.

In addition, the coherence length, as expected, was much shorter for the laser running broad-band than with the birefringent filter inserted. For the narrow-band laser, a stable signal could be obtained over a moderate range of values of the optical delay. By contrast, for the free-running laser, the resolution in our translation stage was barely sufficient to produce a signal. The converse of this, of course, is that the spatial resolution for the broad-band laser will be finer (≈0.1 mm) than for the narrow-band laser (≈1 mm). This variable spatial resolution (and coherence length) can be exploited to simultaneously produce acceptable spatial resolution with good signal stability.

## Publication

Zerkle, D.K., Bigio, I.J., Nogar, N.S., Sappey, A.D., "Imaging Through Turbid Media with a Nonlinear-Optical Correlation Time Gate," OSA TOPS on Advances in Optical Imaging and Photon Migration, **Vol. 2**, pp. 103-107 (1996).

## References


1. K. M. Yoo, B. B. Das, and R. R. Alfano "Imaging of a translucent object hidden in a highly scattering medium from the early portion of the diffuse component of a transmitted ultrafast laser pulse," *Opt. Lett.* **17** , 958-960 (1992).

2. L. Wang *et al*, "Ballistic 2D imaging through scattering walls using an ultrafast Kerr gate," *Science* **253** , 769-771 (1991).

3. L. Wang, P. P. Ho, and R. R. Alfano, "Time-resolved Fourier spectrum and imaging in highly scattering media," *Appl. Opt.* **32** (26), 5043-8 (1993).

4. M. D. Duncan, R. Mahon, L. L. Tankersley, and J. Reintjes, "Time-gated imaging through scattering media using stimulated Raman amplification," *Opt. Lett.* **16**, 1868-1870 (1991).

5. M. Bashkansky *et al*, "Coherently amplified Raman polarization gate for imaging through scattering media," *Opt. Lett.* **19**, 350-352 (1994).

6. J. Reintjes *et al*, "Time-gated imaging with nonlinear optical Raman interactions," *Opt. Photon. News* **4** (10), 28-32 (1993).

7. M. Bashkansky and J. Reintjes, "Imaging through a strong scattering medium with nonlinear-optical field-coherent techniques," *Opt. Lett.* **18**, 2132-2134 (1993).

8. A Rebane, J. Feinberg, "Time-resolved Holography," *Nature* **351**, 378-380, (1991).

9. A. D. Sappey, "Optical imaging through turbid media with a degenerate four-wave mixing correlation time gate," *Appl. Opt.* **33** (36), 8346 (1994).

10. H. Chen *et al.*, "Two-dimensional imaging through diffusing media using 150-fs gated electronic holography techniques," *Opt. Lett.* **16** (7), 487-9 (1991).

11. Y. Chen *et al.*, "Evaluation of holographic methods for imaging through biological tissue," *Appl. Opt.* **32** (23), 4330-4336 (1993).

12. H. Chen *et al.*, "Electronic holographic imaging through living human tissue," *Appl. Opt.* **33** (17), 3630-3632 (1994).

13. A. Costela, J. M. Figuera, and F. Florido, "Thermal and acoustic effects in optical phase conjugation in Rhodamine 6G solutions with nanosecond pulses," *Opt. Commun.* **100** (5-6), 536-44 (1993).

14. J. O. Tocho, W. Sibbett, and D. J. Bradley, "Picosecond phase-conjugate reflection from organic dye saturable absorbers," *Opt. Commun.* **34** (1), 122-6 (1980).

15. H. J. V. Staveren, C. J. M. Moses, J. V. Marle, S. A. Prahl, and M. J. C. V. Gemert, "Light scattering in Intralipid-10% in the wavelength range 400-1100 nm," *Appl. Opt.* **30** (31), 4507-4517 (1991).

16. G. Mitic *et al.*, "Time-gated trans-illumination of biological tissues and tissue like phantoms," *Appl. Opt.* **33** (28), 6699-6710 (1994).

17. H. Key *et al.*, "Optical attenuation characteristics of breast tissues at visible and near-infrared wavelengths," *Phys. Med. Biol.* **36** (5), 579-590 (1991).

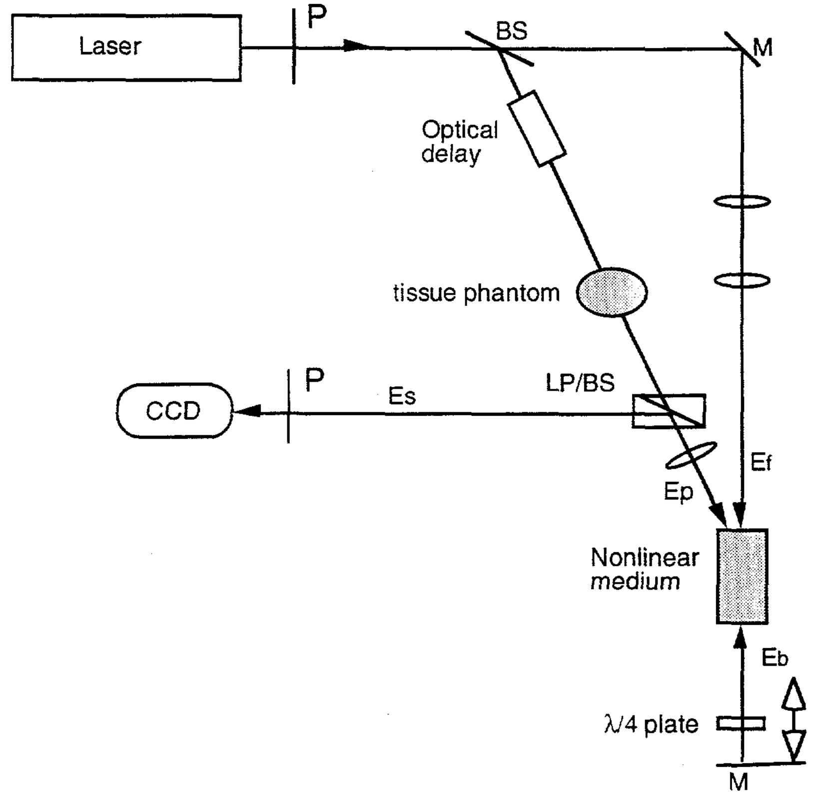


Figure 1. Schematic of the experimental apparatus. The source is a $Cr^{+3}$:$Li_2SrAlF_6$ laser, P are linear polarizers, M are mirrors, BS is a beam splitter, LP/BS is a linear polarizing beamsplitter. $E_f$, $E_b$, $E_p$, are the forward, backreflected, and probe beams, respectively; the optical delay is mounted on a precision translation stage.

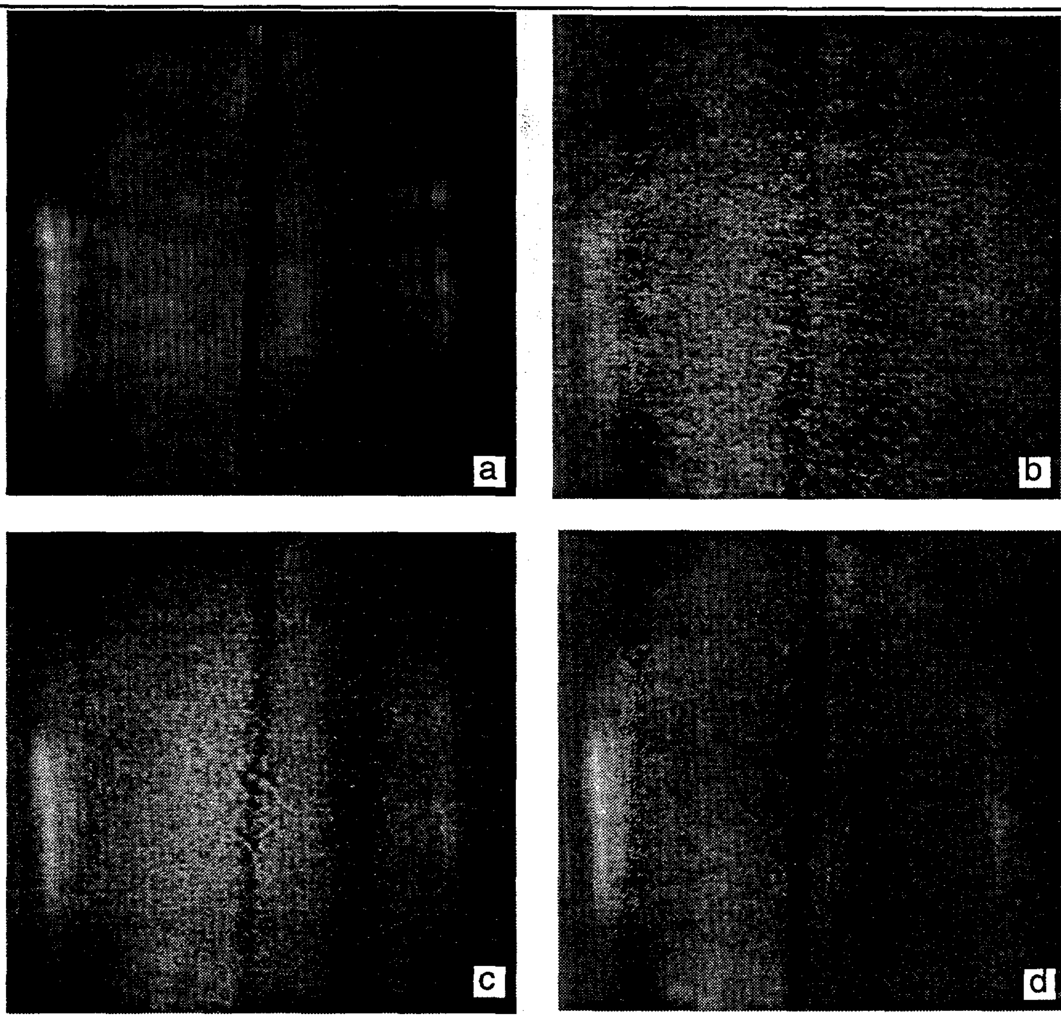


Figure 2. Several images obtained from a 300-μm-diameter crosshair. 2a shows the image resulting from a 10-shot average through a nonscattering medium: 2b, 2c and 2d show, respectively, 10-, 25- and 50-shot averages through a scattering medium.